

Published in final edited form as:

ACS Chem Biol. 2010 September 17; 5(9): 875–885. doi:10.1021/cb100193h.

## A Metabolic Alkene Reporter for Spatiotemporally Controlled Imaging of Newly Synthesized Proteins in Mammalian Cells

Wenjiao Song<sup>†</sup>, Yizhong Wang<sup>†</sup>, Zhipeng Yu<sup>†</sup>, Claudia I. Rivera Vera<sup>†</sup>, Jun Qu<sup>‡</sup>, and Qing Lin<sup>\*,†</sup>

<sup>†</sup>Department of Chemistry, State University of New York at Buffalo, Buffalo, New York 14260

<sup>‡</sup>Department of Pharmaceutical Sciences, State University of New York at Buffalo, Buffalo, New York 14260

### Abstract

The non-symmetrical spatial distribution of newly synthesized proteins in animal cells plays a central role in many cellular processes. Here, we report that a simple alkene tag, homoallylglycine (HAG), was co-translationally incorporated into a recombinant protein as well as endogenous, newly synthesized proteins in mammalian cells with high efficiency. In conjunction with a photoinduced tetrazole-alkene cycloaddition reaction (“photoclick chemistry”), this alkene tag further served as a bioorthogonal chemical reporter both for the selective protein functionalization *in vitro* and for a spatiotemporally controlled imaging of the newly synthesized proteins in live mammalian cells. This two-step metabolic alkene tagging–photo-controlled chemical functionalization approach may offer a potentially useful tool to study the role of the spatiotemporally regulated protein synthesis in mammalian cells.

### Introduction

The use of small organic groups, such as aldehyde/ketone,<sup>1</sup> azide<sup>2</sup> and alkyne,<sup>3</sup> as bioorthogonal chemical reporters for the study of biomolecular dynamics *in vivo* has attracted substantial interests recently.<sup>4</sup> Compared to genetically encoded protein reporters such as green fluorescent protein,<sup>5</sup> the incorporation of chemical reporters are less likely to perturb the folding, localization and thus function of the target protein *in vivo* because of their smaller sizes. Moreover, these chemical reporters could serve as reaction portals where a multitude of biophysical probes can be covalently attached via a growing repertoire of bioorthogonal reactions.<sup>6</sup> For example, an aldehyde/ketone can be selectively conjugated to the hydrazide/alkoxyamine-linked probes via nucleophilic addition; an azide can be selectively functionalized with the alkyne-containing probes via copper(I)-catalyzed “click chemistry”,<sup>7</sup> strained-promoted cycloaddition,<sup>2e–f</sup> and Staudinger ligation<sup>2a</sup>; and conversely, a terminal alkyne can be conjugated with the azide-containing probes via click chemistry. The applications of these bioorthogonal chemical reporters to various classes of biomolecules have led to many new biological insights, including glycan dynamics,<sup>8</sup> enzymatic pathways,<sup>9</sup> protein lipidation,<sup>10</sup> DNA/RNA synthesis,<sup>11</sup> and phospholipid metabolism.<sup>12</sup>

Despite its biological inertness and its rich chemistry in water,<sup>13</sup> the use of an alkene as an intracellular bioorthogonal chemical reporter in mammalian cells has not been reported.

\* qinglin@buffalo.edu .

Supporting Information Available. Additional experimental procedures and characterization data for new compounds. This material is available free of charge via the Internet at <http://pubs.acs.org>.

Whereas several alkene amino acids<sup>14</sup> have been designed and incorporated into proteins site-selectively using either genetic or metabolic approach in *E. coli* and *Saccharomyces cerevisiae*, the methods for the selective functionalization of alkenes in living systems are still scarce. We recently demonstrated that the photoinduced tetrazole-alkene cycloaddition (“photoclick chemistry”) can be employed to functionalize an *O*-allyl-tyrosine-encoded protein in *E. coli* cells.<sup>13c</sup> Besides, Hilderbrand and co-workers reported that *trans*-cyclooctene could serve as a bioorthogonal chemical reporter for selective imaging of cancer cells in which *trans*-cyclooctene was first attached to an anti-EGFR antibody and then reacted with a tetrazine reagent *via* an inverse-electron-demand Diels-Alder reaction.<sup>15</sup> Because of its large size, it remains to be investigated whether *trans*-cyclooctene can be genetically encoded into biomolecules site-selectively.

Alkene functionality is naturally present in mammalian cells, with the vast majority in the form of internal *cis*-alkenes found in phospholipids and a small fraction in the unsaturated lipid-derived signaling molecules such as sphingosine 1-phosphate, anandamide, linoleic acid, retinoic acid, and farnesyl pyrophosphate. We envision that an exogenous terminal alkene can serve as a viable bioorthogonal chemical reporter because: (1) most endogenous alkene groups are not accessible to chemical reactions due to the fact that they are tightly packed in lipid membranes; (2) the exogenous terminal alkenes are more reactive than internal alkenes in the photoclick chemistry.<sup>16</sup> Here, we report the first incorporation of a metabolic alkene reporter, homoallylglycine (HAG), into proteins in mammalian cells, and the utility of this alkene reporter in the spatiotemporally controlled imaging of the newly synthesized proteins via photoclick chemistry in live mammalian cells (Figure 1).

## Results and Discussion

### Metabolic Incorporation of HAG into Mammalian Proteins

Since HAG represents the simplest terminal alkene and has shown co-translational activity in a bacterial methionine auxotrope,<sup>14c</sup> we reasoned that HAG should serve as a methionine surrogate for co-translational incorporation in mammalian cells as well because: (1) mammalian cells lack the methionine biosynthetic machinery;<sup>17</sup> (2) human methionyl-<sup>t</sup>RNA synthetase shares high homology with its *E. coli* ortholog,<sup>18</sup> and (3) similar methionine surrogates such as azidohomoalanine (AHA) and homopropargylglycine (HPG) have successfully employed by Tirrell and Schuman to identify and image the newly synthesized proteins in neurons.<sup>2f</sup> 19 To examine whether HAG can be co-translationally incorporated into mammalian proteins, HeLa cells were cultured in the methionine-deficient DMEM medium supplemented with HAG, and the HAG incorporation into the newly synthesized proteins was probed by in-gel fluorescence analysis of the freshly prepared cell lysates after the photoinduced cycloaddition reaction with tetrazole **1** (Table 1).<sup>20</sup> Using the fluorescence intensity to quantify the extent of HAG incorporation, we found that the highest incorporation efficiency was obtained when cells were cultured in the presence of 1 mM HAG for about 20 hr (Figure 2). Importantly, the cell proliferation assay as determined by hemacytometer (Table S1 in the Supporting Information) and the CellTiter-Glo based cell viability assay (Figure S2 in the Supporting Information) indicated that the HAG labeling procedure did not cause cytotoxicity during the incubation periods. Furthermore, treatment of HeLa cells with either anisomycin (40  $\mu$ M) or cycloheximide (50  $\mu$ M) for 30 min prior to the HAG labeling completely abolished the incorporation of HAG into the cellular proteins (Figure S3), indicating that indeed HAG only labels the newly synthesized proteins.<sup>21</sup>

### HAG Occupancy in Mammalian Proteins

To determine the HAG occupancy at the different Met sites, we overexpressed a C-terminal His-tagged  $\beta$ -galactosidase ( $\beta$ -gal) by transiently transfecting 293T cells with pcDNA4/myc-

His/lacZ plasmid and allowed protein expression to proceed in the methionine-deficient HAG labeling medium. The HAG-encoded  $\beta$ -gal was purified by using the Ni-NTA beads and subsequently digested with trypsin and V8 to generate the peptide fragments. The HAG presence in these fragments was then analyzed by nanoLC-tandem mass spectrometry. Based on 19.97-Da mass reduction relative to Met in the MS2 spectra (Figure S4), 12 unique HAG substitutions were unambiguously identified among 24 Met sites (Table 2). Gratifyingly, 10 corresponding Met-encoding peptide fragments were also positively identified (entries 1–10 in Table 2). Using ion count as an approximation for fragment abundance, we calculated the HAG occupancy based on the following equation: % occupancy =  $I_{\text{HAG}}/(I_{\text{HAG}} + I_{\text{Met}})$ , where  $I_{\text{HAG}}$  and  $I_{\text{Met}}$  are ion counts for the HAG- and Met-encoded peptide fragments in the MS spectra, respectively (Figure S5). We found the HAG occupancy in  $\beta$ -gal varied in the range of 42–85% (Table 2), with no apparent structure-occupancy relationship after mapping the identified HAG sites onto the  $\beta$ -gal structure (Figure S6). This finding is consistent with the co-translational nature of HAG incorporation in which HAG is activated by a methionyl-tRNA synthetase and charged into a growing polypeptide chain during the ribosomal synthesis when the polypeptide has yet to fold into a globular structure. The differences in HAG occupancy are generally less than two-fold, which can be attributed to variations in ionization potential among 20 HAG- and Met-encoded peptide fragments.

### Effect of HAG Incorporation on Protein Function *In Vitro*

While Met occurrence in protein is relatively low (~1.8%),<sup>22</sup> substantial global displacement of Met by HAG nevertheless raises a critical concern that it may potentially alter the folding and thus function of the HAG-encoded proteins. To alleviate this concern, we compared the enzymatic activity of the HAG-encoded  $\beta$ -gal to that of wild-type (wt) in the cell lysates. Using *ortho*-nitrophenyl- $\beta$ -galactoside (ONPG) as a chromogenic substrate, in the kinetic assay the HAG-encoded  $\beta$ -gal showed a maximum velocity ( $V_{\text{max}}$ ) of  $0.0357 \pm 0.0011$  AU/min, essentially identical to that of wt- $\beta$ -gal ( $V_{\text{max}} = 0.0378 \pm 0.0006$  AU/min) (Figure S7a). Importantly, the expression levels of HAG- and wt- $\beta$ -gal in the cell lysates were found to be identical by the western blot analysis using an anti-myc antibody (Figure S7b). This result confirmed that HAG substitutions did not significantly affect the  $\beta$ -gal enzymatic activity. Since  $\beta$ -gal functions as a tetramer,<sup>23</sup> this result also implies that HAG substitutions did not disrupt its tetramerization. The kinetic finding is consistent with the cell proliferation and viability assay results in which no HAG-related cytotoxicity was detected where cells were grown in the HAG supplemented medium.

### HAG for Protein Modification *In Vitro*

To examine whether the metabolically incorporated HAG can be selectively functionalized with the tetrazole reagents, first, we reacted the purified HAG- and wt- $\beta$ -gal, respectively, with 2 mM tetrazole **1** and found only HAG- $\beta$ -gal showed the formation of the fluorescent pyrazoline band on the SDS-PAGE gel (Figure 3a). The reaction yield was estimated to be  $56 \pm 14\%$ , as determined by quantifying the fluorescence intensity (Figure S8). To examine whether the HAG-encoded cell lysate undergoes selective cycloaddition reaction, we incubated BODIPY-tetrazole **2** (see Table 1 for structure) with the HAG-encoded or normal cell lysate and tracked the reactions *via* BODIPY fluorescence on the gel. We found that only the HAG-encoded cell lysate was selectively labeled with the green BODIPY dye (Figure 3b, middle panel). Similarly, when the HAG-encoded cell lysate was incubated with biotin-tetrazole **3** (see Table 1 for structure) the biotinylated products can be detected by streptavidin-alkaline phosphatase in a western blot (Figure 3b, right panel). Taken together, these results confirmed that HAG can serve as a viable bioorthogonal chemical reporter for selective protein modification *in vitro* by the tetrazole-derived probes.

## HAG for Protein Labeling in Live Cells

To examine whether HAG represents a suitable tag for labeling newly synthesized proteins in living cells, HAG-labeled HeLa cells were suspended in 1 mL PBS buffer containing either 500  $\mu$ M tetrazole **4** (used because of its superior fluorescence quantum yield; see Table 1) or 5% DMSO. After 10-min incubation at 37 °C, the cells were exposed to a 302-nm UV light for 5 min before additional 4 mL PBS buffer was added. The cells were then directly analyzed by fluorescence activated cell sorting (FACS) using a 407-nm violet laser for excitation and a 450/50 bandpass filter for fluorescence detection. We found that after the photoinduced reaction the HAG-labeled HeLa cells showed significantly greater increase in fluorescent cell population than the normal HeLa cells (Figure 4a). Quantification of the histograms showed that the HAG-labeled cells yielded 11-fold increase in mean fluorescence compared to the DMSO control (Figure 4b). By contrast, the unlabeled cells showed about 3-fold increase in mean fluorescence after the reaction compared to the DMSO control. The increased background fluorescence seen in normal HeLa cells can be attributed to the intracellular retention of tetrazole **4**, which produces the weakly fluorescent nitrile imine intermediate upon laser activation (407 nm) during the flow cytometric analysis (see Figure S9 for fluorescence spectrum of the nitrile imine intermediate). Nevertheless, the roughly 4-fold increase in mean fluorescence detected in the HAG-labeled cells over normal cells suggests that HAG can serve as a useful chemical tag.

The selective photoinduced cycloaddition reaction with the HAG-labeled HeLa cells was further confirmed by fluorescent microscopy (Figure 5). In this experiment, the HAG-labeled cells grown on cover slips were treated with 100  $\mu$ M tetrazole **4** for 10 min followed by exposure to 302-nm handheld UV light for 2 min. The cells were then washed with PBS and examined by fluorescent microscopy. In the DAPI channel (ex 365 nm, em 445  $\pm$  25 nm), the HAG-labeled HeLa cells showed strong fluorescence while normal HeLa cells did not (Figure 5a, top panels), indicating that the reaction was selective. There was no significant treatment-related cellular toxicity based on the DIC images (Figure 6a, bottom panels) and the cell viability assay (Figure S10). To verify that the observed fluorescence arose from the cycloaddition reaction with the newly synthesized proteins, the treated cells were lysed after photo-exposure and the lysates were subjected to in-gel fluorescence analysis. Only the HAG-encoded cell lysate showed fluorescent protein bands while the unlabeled cell lysate did not (Figure 5b), indicating that cellular fluorescence was indeed due to the formation of pyrazoline protein adducts.

## Spatiotemporally Controlled Imaging of Proteins in Live Cells

The main advantage of using an alkene reporter along with photoclick chemistry for protein imaging is the potential of spatiotemporal control. To demonstrate this, the HAG-labeled HeLa cells grown on a glass cover-slip in a sealed chamber were incubated with 200  $\mu$ M of a 365-nm photoactivatable tetrazole **5** (Table 1).<sup>24</sup> After briefly exposing the cells to a two-photon 700 nm laser (5 sec), the cellular fluorescence was recorded over 1 min with a confocal microscope equipped with a DAPI filter. We found only the directly illuminated HAG-HeLa cell showed a rapid and more than 2-fold increase in fluorescence relative to the unilluminated cells (Figure 6a, top row; Figure 6b, left plot), indicating a temporal and spatial resolution can be achieved with the HAG reporter. As a control, a slight increase in fluorescence was observed for the illuminated normal HeLa cell, which was indistinguishable from the non-illuminated normal cells (Figure 6a, bottom row; Figure 6b, right plot). Similar to what we observed in the FACS analysis (Figure 4), the increased background fluorescence seen with normal cells was likely due to the photo-generated, weakly fluorescent nitrile imine intermediate.

Compared to direct incorporation of biophysical probes into proteins, co-translational incorporation of HAG followed by its selective functionalization offers several unique advantages in tracking protein dynamics in living cells. First, this two-step approach gets around the size constraint imposed by the methionyl-<sup>1</sup>RNA synthetase on the amino acid surrogate sidechains. Importantly, the co-translational incorporation efficiency of HAG was found to be rather high, in the range of 42–85% based on a mass-spectrometry analysis (Table 2). Secondly, the incorporation of HAG did not seem to significantly perturb protein folding, structure, and likely subcellular localization. There was no apparent cytotoxicity when HAG was incorporated into many cellular proteins (Figure S2). In the kinetic analysis of the HAG- and Met-encoded  $\beta$ -galactosidase, no difference in  $V_{\max}$  was detected (Figure S7). Thirdly, HAG served as a reaction portal where diverse small-molecule probes such as fluorescence and affinity probes were attached through the photoclick chemistry *in vitro* (Figure 3) and *in vivo* (Figures 4–6). Fourth, the labeling procedure was straightforward and in principle applicable to tissue samples and living organisms because there was no genetic manipulation involved.

Compared to the recently reported photo-triggered copper-free azide-alkyne cycloaddition,<sup>25</sup> which clearly has a potential in functionalizing azide-containing biomolecules with a spatiotemporal resolution, this alkene reporter–photoclick chemistry strategy generates fluorescent adducts *in situ* rapidly (in seconds) and thus allows the monitoring of the newly synthesized proteins in real time without the need of washing (e.g., in Figure 6). This streamlined procedure is particularly advantageous when the repeated washings are not feasible, e.g., in higher living organisms.

## Conclusion

In summary, we have shown that a simple alkene amino acid, HAG, can serve as a useful metabolic reporter for newly synthesized proteins both *in vitro* and *in vivo*. The HAG metabolic labeling procedure was straightforward, and the incorporation efficiency was high with occupancies in the range of 42% to 85%. Importantly, the HAG metabolic labeling did not appear to disrupt protein function, as evidenced both by the kinetic analysis and the devoid of cytotoxicity during the cell culture. In conjunction with the photoinduced tetrazole-alkene cycloaddition reaction, the HAG-encoded proteins can be modified with a variety of tetrazole reagents *in vitro*. Furthermore, this bioconjugation chemistry can be carried out in intact cells, allowing the labeled cells to be sorted by flow cytometry. Finally, we demonstrated that the HAG reporter can be used to image the newly synthesized proteins in mammalian cells with spatiotemporal control. The efforts to increase the sensitivity of this labeling chemistry and apply this technique to study spatial cell biology<sup>26</sup> are currently underway.

## Experimental Section

### Metabolic Labeling of HeLa Cells with HAG

HeLa cells were allowed to grow to 80–90% confluency on a 35-mm tissue culture plate in DMEM medium supplemented with 10% FBS. After removing the medium, the cells were washed twice with pre-warmed DPBS (3 mL each) before 3 mL of pre-warmed methionine-deficient DMEM medium was added. The cells were incubated in a humidified 37 °C, 5% CO<sub>2</sub> incubator for 30 min to deplete the intracellular methionine pool. The medium was then removed and a fresh 2-mL labeling medium (DMEM, 10% dialyzed FBS, -Met, 0.1–2 mM HAG used in the concentration-dependency study; 1 mM HAG used in the time-course study) was added before the plate was returned to CO<sub>2</sub> incubator for the indicated time (8 hr for the concentration-dependency study and 1 ~ 28 hr for the time-course study). After



metabolic labeling, the medium was removed and the cells were washed twice with 3 mL of ice-cold PBS. The HAG-labeled cells were then used in the subsequent studies.

### Determining HAG Incorporation Efficiency

To a 35-mm tissue culture plate containing confluent HAG-labeled HeLa cells was added 100  $\mu$ L of ice-cold lysis buffer (10 mM Tris, 50 mM NaCl, 30 mM sodium pyrophosphate, 50 mM NaF, 5 mM EDTA, and 0.1 mM  $\text{Na}_3\text{VO}_4$ , 1% Triton X-100, pH 7.6) and the plate was placed on ice for 20 min. The cells were then dislodged from the plate surface and the lysate was collected and centrifuged at  $16,000 \times g$  at 4 °C for 30 min. The supernatant was transferred to a new eppendorf tube. To set up the reactions, 20  $\mu$ L of cell lysates were mixed with 1  $\mu$ L of tetrazole **1** (40 mM in DMSO) in a 96-well microtiter plate. After irradiating the mixtures with a handheld 302-nm UV lamp for 10 min, the reactions were quenched by adding 4  $\mu$ L of 6 $\times$  SDS sample buffer and boiled at 95 °C for 5 min. The samples were then loaded onto a precast NuPAGE 4–12% Bis-Tris gel (Invitrogen) and subjected to protein electrophoresis. The fluorescent bands in the gel were recorded with a digital camera by illuminating the gel with a handheld 365-nm UV lamp. Subsequently, the same gel was stained with Coomassie Blue to reveal the sizes and equal loading of proteins. The fluorescence intensities were quantified using the NIH ImageJ program.

### Purifying HAG-Encoded and Wild-Type $\beta$ -Galactosidases

To overexpress  $\beta$ -galactosidase in mammalian cells, human embryonic kidney (HEK) 293T cells were grown on 10-cm tissue culture plates. Lipofectamine 2000 was used to transiently transfect 293T cells with the pcDNA4/myc-His/lacZ plasmid (Invitrogen). After 20–24 hr, the medium was switched to the HAG (1 mM) labeling medium or regular DMEM medium for another 48 hr. The cells were then rinsed with DPBS to remove HAG before a treatment of 0.5 mL lysis buffer (50 mM Tris, 300 mM NaCl, 1% NP-40, protease inhibitor cocktail, pH 7.8). The lysates were subjected to three freeze-thaw cycles and centrifuged at  $16,000 \times g$  at 4 °C for 30 min. The  $\beta$ -galactosidases in the supernatant were extracted with Ni-NTA beads (Sigma, St. Louis, MO) by following the manufacturer's instructions. The purified protein was desalted using Protein Desalting Spin Columns (PIERCE, Rockford, IL).

### ONPG-Based $\beta$ -Gal Activity Assay

To 5  $\mu$ L cell lysates containing either HAG-encoded or wild-type  $\beta$ -galactosidase were added 1 mL of freshly prepared *ortho*-nitrophenyl- $\beta$ -galactoside (ONPG) solution (3 mM in PBS, 10 mM  $\text{MgCl}_2$ , 0.1 mM 2-mercaptoethanol, pH 7.5). The UV absorbance at 420 nm was recorded at various times over a period of 12 min. The maximum velocities ( $V_{\text{max}}$ ) were derived by least-square fitting of all data points to a linear equation. To confirm equal amounts of  $\beta$ -galactosidases present in the cell lysates, the protein mixtures in the cell lysates were resolved by SDS-PAGE, and the  $\beta$ -galactosidase was detected by western blot using an anti-Myc antibody (Invitrogen, Carlsbad, CA).

### Reactions of HAG-Encoded $\beta$ -Gal with Tetrazole

To 20- $\mu$ L PBS buffer containing the purified  $\beta$ -gal (0.12 g, 0.11  $\mu$ M final concentration) and 2.0 M urea was added 1  $\mu$ L tetrazole **1** (2 mM final concentration). The mixture was irradiated with a handheld 302-nm UV light for 5 min. The samples were then loaded onto a NuPAGE 4–12% Bis-Tris gel for SDS-PAGE. The resolved gel was subjected to both Coomassie blue staining and in-gel fluorescence analysis. The amount of  $\beta$ -gal pyrazoline adducts was determined by comparing its fluorescence intensity to that of a 5-kDa mPEG-pyrazoline with known concentrations on the same gel. The yield of the cycloaddition was estimated by assuming 50% HAG occupancy at all 24 methionine sites.

## Functionalization of HAG-labeled Cell Lysates

For BODIPY modification, 20  $\mu$ L of HAG-labeled 293T cell lysate (or the Met control) was incubated with 2  $\mu$ L BODIPY-tetrazole **2** (20 mM in DMSO) in PBS buffer. After irradiating the mixtures in a 96-well microtiter plate with a handheld 302-nm UV lamp for 20 min and additional incubation at room temperature for 1.5 hr, the reactions were quenched by adding 1  $\mu$ L of 1 N HCl. After adjusting pH to 7.0 with 1 N NaOH, 5  $\mu$ L of 6 $\times$  SDS sample buffer was added and the mixtures were boiled at 95  $^{\circ}$ C for 5 min. The samples were loaded onto a NuPAGE 4–12% Bis-Tris gel and resolved by protein electrophoresis. The resolved gel was subjected to both Coomassie blue staining and in-gel fluorescence analysis. For biotinylation, 20  $\mu$ L solution of HAG-labeled 293T cell lysate (or Met control) was incubated with 2  $\mu$ L biotin-tetrazole **3** (200  $\mu$ M in DMSO) and 1  $\mu$ L TCEP (30 mM in ddH<sub>2</sub>O) in PBS buffer. After irradiating the mixtures in a 96-well microtiter plate with a handheld 302-nm UV lamp for 5 min followed by incubation at room temperature for 1.5 hr, the reactions were quenched by adding 1  $\mu$ L of 1 N HCl. After adjusting pH to 7.0 with 1 N NaOH, 5  $\mu$ L of 6 $\times$  SDS sample buffer was added and the mixtures were boiled at 95  $^{\circ}$ C for 5 min. The samples were loaded onto a NuPAGE 4–12% Bis-Tris gel and subjected to protein electrophoresis. The proteins were then transferred to the PDVF membrane (Millipore, Bedford, MA) using a semi-dry protein transfer apparatus and blotted with the VECTASTAIN ABC-AmP reagent kit (Vector Laboratories, Burlingame, CA) by following the manufacturer's instructions.

## Fluorescence Activated Cell Sorting

HeLa cells were allowed to grow to 80–90% confluency on the 10-cm tissue culture plates. After metabolic labeling of HAG overnight, the labeled cells and the Met control cells were detached from plate surfaces by treatment of 10 mL of 0.25% trypsin-EDTA containing DMEM medium and collected by centrifugation at  $300 \times g$  for 5 min at room temperature. The pellets were washed twice with PBS, and re-suspended in 1 mL PBS buffer containing either 500  $\mu$ M of tetrazole **4** or 5% DMSO. After incubation at 37  $^{\circ}$ C for 10 min, the cells were irradiated with a handheld 302-nm UV lamp for 5 min before dilution with 4 mL PBS. The cells were then subjected to FACS analysis using a BD LSR II flow cytometer (BD Biosciences, San Jose, CA). Cells were excited with a 407-nm violet laser and cellular fluorescence were detected using a 450/50 bandpass filter. A total of 20,000 events were collected for each sample and the forward- and side-scatter properties were used to exclude doublets, dead cells, and debris during analysis. The error bars represent standard deviations from three independent measurements.

## Live Cell Fluorescent Imaging

HeLa cells were allowed to grow to 60–70% confluency on cover-slips placed in the tissue culture plates. After metabolic labeling of HAG overnight under the optimized conditions, the HAG-labeled cells and the Met control cells were treated with tetrazole **4** (100  $\mu$ M, 5% DMSO in PBS buffer) for 10 min, followed by photoirradiation with a handheld 302-nm UV lamp for 2 min. After washing twice with PBS, the cover-slide was flipped and placed on top of a glass slide installed with *In situ*-Frame to make a sealed sample chamber containing PBS buffer. The sample was then placed underneath fluorescent microscope for imaging acquisition. Subsequently, roughly  $1 \times 10^5$  labeled cells were lysed by adding 10  $\mu$ L 6 $\times$  SDS sample buffer and boiled at 95  $^{\circ}$ C for 5 min. The samples were then loaded onto a NuPAGE 4–12% Bis-Tris gel and resolved by protein electrophoresis. The fluorescent bands in the gel were recorded with a digital camera by illuminating the gel with a handheld 365-nm UV lamp. The same gel was stained with Coomassie Blue to reveal the sizes and amounts of proteins loaded onto the gel.

## Two-Photon Fluorescent Imaging

HeLa cells were allowed to grow to 30–40% confluency on cover-slips placed inside the tissue culture plates. After metabolic labeling of HAG overnight under the optimized condition, the HAG-labeled cells and the Met control cells were washed twice with pre-warmed PBS. The cover-slip was flipped and placed on top of a glass slide installed with *In situ*-Frame to make a sealed sample chamber containing tetrazole **5** (200  $\mu$ M, 2% DMSO in PBS buffer). The sample was placed underneath the confocal microscope for the two-photon initiated reaction and subsequent imaging acquisitions. The imaging acquisitions were carried out using a Zeiss LSM-510 meta-NLO System equipped with a Coherent Chameleon Ultra II Ti/Sapphire laser and external non-descanned detectors and specifically configured for multi-photon imaging. The laser power was set at 7% for reaction initiation and 1.6% for imaging acquisition. A Plan-Apochromat 63 $\times$ /1.4 oil DIC objective was used. The two-photon laser excitation wavelength was set at 700 nm, and the DAPI filter set (435–485 nm) was used in the fluorescence capture. The data quantification was carried out using the software installed in LSM-510.

## Supplementary Material

Refer to Web version on PubMed Central for supplementary material.

## Acknowledgments

We gratefully acknowledge the National Institute of General Medical Sciences, the National Institutes of Health (GM85092) and SUNY Buffalo IRDF for financial support. We thank Dr. Wade Sigurdson at SUNY Buffalo Confocal Microscopy Facility for his assistance in fluorescent microscopy.

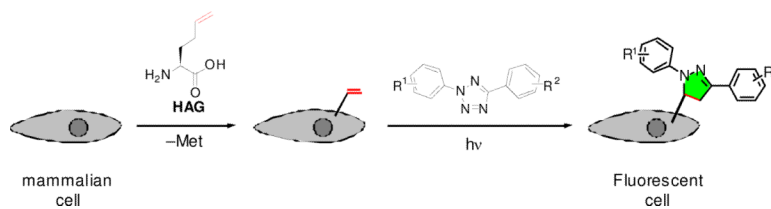
## REFERENCES

- (1). (a) Mahal LK, Yarema KJ, Bertozzi CR. Engineering chemical reactivity on cell surfaces through oligosaccharide biosynthesis. *Science*. 1997; 276:1125–1128. [PubMed: 9173543] (b) Chen I, Howarth M, Lin W, Ting AY. Site-specific labeling of cell surface proteins with biophysical probes using biotin ligase. *Nat. Methods*. 2005; 2:99–104. [PubMed: 15782206] (c) Carrico IS, Carlson BL, Bertozzi CR. Introducing genetically encoded aldehydes into proteins. *Nat. Chem. Biol.* 2007; 3:321–322. [PubMed: 17450134] (d) Zeng Y, Ramya TN, Dirksen A, Dawson PE, Paulson JC. High-efficiency labeling of sialylated glycoproteins on living cells. *Nat. Methods*. 2009; 6:207–209. [PubMed: 19234450]
- (2). (a) Saxon E, Bertozzi CR. Cell surface engineering by a modified Staudinger reaction. *Science*. 2000; 287:2007–2010. [PubMed: 10720325] (b) Speers AE, Adam GC, Cravatt BF. Activity-based protein profiling in vivo using a copper(i)-catalyzed azide-alkyne [3 + 2] cycloaddition. *J. Am. Chem. Soc.* 2003; 125:4686–4687. [PubMed: 12696868] (c) Hang HC, Yu C, Kato DL, Bertozzi CR. A metabolic labeling approach toward proteomic analysis of mucin-type O-linked glycosylation. *Proc. Natl. Acad. Sci. USA*. 2003; 100:14846–14851. [PubMed: 14657396] (d) Link AJ, Tirrell DA. Cell surface labeling of *Escherichia coli* via copper(I)-catalyzed [3+2] cycloaddition. *J. Am. Chem. Soc.* 2003; 125:11164–11165. [PubMed: 16220915] (e) Agard NJ, Prescher JA, Bertozzi CR. A strain-promoted [3 + 2] azide-alkyne cycloaddition for covalent modification of biomolecules in living systems. *J. Am. Chem. Soc.* 2004; 126:15046–15047. [PubMed: 15547999] (f) Dieterich DC, Link AJ, Graumann J, Tirrell DA, Schuman EM. Selective identification of newly synthesized proteins in mammalian cells using bioorthogonal noncanonical amino acid tagging (BONCAT). *Proc. Natl. Acad. Sci. USA*. 2006; 103:9482–9487. [PubMed: 16769897] (g) Laughlin ST, Baskin JM, Amacher SL, Bertozzi CR. In vivo imaging of membrane-associated glycans in developing zebrafish. *Science*. 2008; 320:664–667. [PubMed: 18451302] (h) Laughlin ST, Bertozzi CR. In vivo imaging of *Caenorhabditis elegans* glycans. *ACS Chem. Biol.* 2009; 4:1068–1072. [PubMed: 19954190]
- (3). (a) Deiters A, Cropp TA, Mukherji M, Chin JW, Anderson JC, Schultz PG. Adding amino acids with novel reactivity to the genetic code of *saccharomyces cerevisiae*. *J. Am. Chem. Soc.* 2003;

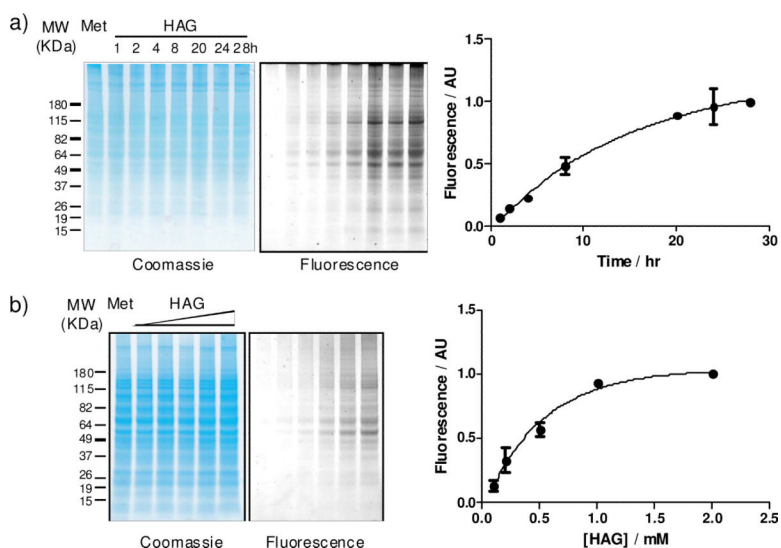


- 125:11782–11783. [PubMed: 14505376] (b) Beatty KE, Liu JC, Xie F, Dieterich DC, Schuman EM, Wang Q, Tirrell DA. Fluorescence visualization of newly synthesized proteins in mammalian cells. *Angew. Chem. Int. Ed.* 2006; 45:7364–7367.
- (4). (a) Best MD. Click chemistry and bioorthogonal reactions: unprecedented selectivity in the labeling of biological molecules. *Biochemistry.* 2009; 48:6571–6584. [PubMed: 19485420] (b) Sletten EM, Bertozzi CR. Bioorthogonal chemistry: fishing for selectivity in a sea of functionality. *Angew. Chem. Int. Ed.* 2009; 48:6974–6998.
- (5). Tsien RY. Constructing and exploiting the fluorescent protein paintbox (Nobel Lecture). *Angew. Chem. Int. Ed.* 2009; 48:5612–5626.
- (6). Lim RKV, Lin Q. Bioorthogonal chemistry: recent progress and future directions. *Chem. Comm.* 2010; 46:1489–1600.
- (7). (a) Rostovtsev VV, Green LG, Fokin VV, Sharpless KB. A stepwise Huisgen cycloaddition process: Copper(I)-catalyzed regioselective “ligation” of azides and terminal alkynes. *Angew. Chem., Int. Ed.* 2002; 41:2596–2599. (b) Torne CW, Christensen C, Meldal M. Peptidotriazoles on solid phase: [1,2,3]-triazoles by regioselective copper(I)-catalyzed 1,3-dipolar cycloadditions of terminal alkynes to azides. *J. Org. Chem.* 2002; 67:3057–3064. [PubMed: 11975567]
- (8). Agard NJ, Bertozzi CR. Chemical approaches to perturb, profile, and perceive glycans. *Acc. Chem. Res.* 2009; 42:788–797. [PubMed: 19361192]
- (9). Barglow KT, Cravatt BF. Activity-based protein profiling for the functional annotation of enzymes. *Nat. Methods.* 2007; 4:822–827. and references therein. [PubMed: 17901872]
- (10). Charron G, Wilson J, Hang HC. Chemical tools for understanding protein lipidation in eukaryotes. *Curr. Opin. Chem. Biol.* 2009; 13:382–391. and references therein. [PubMed: 19699139]
- (11). (a) Salic A, Mitchison TJ. A chemical method for fast and sensitive detection of DNA synthesis in vivo. *Proc. Natl. Acad. Sci. USA.* 2008; 105:2415–2420. [PubMed: 18272492] (b) Jao CY, Salic A. Exploring RNA transcription and turnover in vivo by using click chemistry. *Proc. Natl. Acad. Sci. USA.* 2008; 105:15779–15784. [PubMed: 18840688]
- (12). (a) Neef AB, Schultz C. Selective fluorescence labeling of lipids in living cells. *Angew. Chem. Int. Ed.* 2009; 48:1498–1500. (b) Jao CY, Roth M, Welti R, Salic A. Metabolic labeling and direct imaging of choline phospholipids in vivo. *Proc. Natl. Acad. Sci. USA.* 2009; 106:15332–15337. [PubMed: 19706413]
- (13). (a) de Araújo AD, Palomo JM, Cramer J, Köhn M, Schröder H, Wacker R, Niemeyer C, Alexandrov K, Waldmann H. Diels-Alder ligation and surface immobilization of proteins. *Angew. Chem. Int. Ed.* 2006; 45:296–301. (b) Lin YA, Chalker JM, Floyd N, Bernardes GJ, Davis BG. Allyl sulfides are privileged substrates in aqueous cross-metathesis: application to site-selective protein modification. *J. Am. Chem. Soc.* 2008; 130:9642–9643. [PubMed: 18593118] (c) Song W, Wang Y, Qu J, Lin Q. Selective functionalization of a genetically encoded alkene-containing protein via “photoclick chemistry” in bacterial cells. *J. Am. Chem. Soc.* 2008; 130:9654–9655. [PubMed: 18593155] (d) Blackman ML, Royzen M, Fox JM. Tetrazine ligation: fast bioconjugation based on inverse-electron-demand Diels-Alder reactivity. *J. Am. Chem. Soc.* 2008; 130:13518–13519. [PubMed: 18798613] (e) Devaraj NK, Weissleder R, Hilderbrand SA. Tetrazine-based cycloadditions: application to pretargeted live cell imaging. *Bioconjugate Chem.* 2008; 19:2297–2299.
- (14). (a) van Hest JC, Kiick KL, Tirrell DA. Efficient Incorporation of Unsaturated Methionine Analogues into Proteins in Vivo. *J. Am. Chem. Soc.* 2000; 122:1282–1288. (b) Zhang Z, Wang L, Brock A, Schultz PG. The selective incorporation of alkenes into proteins in *Escherichia coli*. *Angew. Chem. Int. Ed.* 2002; 41:2840–2842. (c) Wang J, Schiller SM, Schultz PG. A biosynthetic route to dehydroalanine-containing proteins. *Angew. Chem. Int. Ed.* 2007; 46:6849–6851. (d) Yanagisawa T, Ishii R, Fukunaga R, Kobayashi T, Sakamoto K, Yokoyama S. Multistep engineering of pyrrolysyl-tRNA synthetase to genetically encode N(epsilon)-(o-azidobenzoyloxycarbonyl) lysine for site-specific protein modification. *Chem. Biol.* 2008; 15:1187–1197. [PubMed: 19022179] (e) Ai H, Shen W, Brustad E, Schultz PG. Genetically encoded alkenes in yeast. *Angew. Chem. Int. Ed.* 2010; 49:935–937.

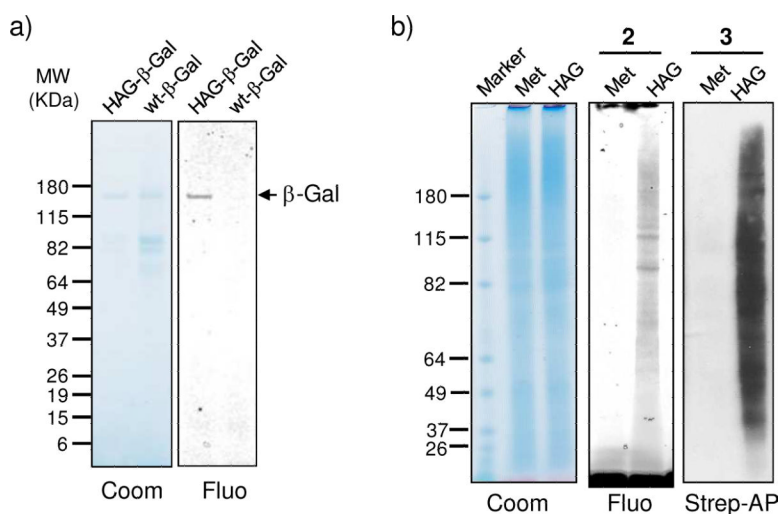
- (15). Devaraj NK, Upadhyay R, Haun JB, Hilderbrand SA, Weissleder R. Fast and sensitive pretargeted labeling of cancer cells through a tetrazine/trans-cyclooctene cycloaddition. *Angew. Chem. Int. Ed.* 2009; 48:7013–7016.
- (16). Huisgen R, Knupfer H, Sustmann R, Wallbillich G, Weberndorfer V. 1,3-Dipolar cycloadditions. XXVII. Addition of diphenylnitrilimine to nonconjugate alkenes and alkynes. Steric course of reaction, orientation, and effect of substituents. *Chem. Ber.* 1967; 100:1580–1592. (b) We subjected a mixture of 2-phenyl-5-(*p*-methoxy)phenyl-tetrazole, 4-penten-1-ol, *cis*-4-hexen-1-ol, and *trans*-4-hexen-1-ol in 3:1 acetonitrile/PBS buffer to 302-nm UV irradiation for 3 hr, and found that 4-penten-1-ol afforded six times more cycloadduct than *trans*-4-hexen-1-ol while *cis*-4-hexen-1-ol did not give any cycloadduct: see Figure S1 in the Supporting Information for details.
- (17). Coligan JE, Gates FT, Kimball ES, Maloy WL. Radiochemical sequence analysis of metabolically labeled proteins. *Methods Enzymol.* 1983; 91:413–434. [PubMed: 6343759]
- (18). Serre L, Verdon G, Choinowski T, Hervouet N, Risler J-L, Zelwer C. How methionyl-tRNA synthetase creates its amino acid recognition pocket upon L-methionine binding. *J. Mol. Biol.* 2001; 306:863–876. [PubMed: 11243794]
- (19). Dieterich DC, Hodas JJ, Gouzer G, Shadrin IY, Ngo JT, Triller A, Tirrell DA, Schuman EM. In situ visualization and dynamics of newly synthesized proteins in rat hippocampal neurons. *Nat. Neurosci.* 2010; 13:897–905. [PubMed: 20543841]
- (20). Wang Y, Song W, Hu WJ, Lin Q. Fast alkene functionalization in vivo by Photoclick chemistry: HOMO lifting of nitrile imine dipoles. *Angew. Chem. Int. Ed.* 2009; 48:5330–5333.
- (21). Beatty KE, Tirrell DA. Two-color labeling of temporally defined protein populations in mammalian cells. *Bioorg. Med. Chem. Lett.* 2008; 18:5995–5999. [PubMed: 18774715]
- (22). Lathe R. Synthetic oligonucleotide probes deduced from amino acid sequence data. Theoretical and practical considerations. *J. Mol. Biol.* 1985; 183:1–12. [PubMed: 4009718]
- (23). Matthews BW. The structure of *E. coli* beta-galactosidase. *C. R. Biol.* 2005; 328:549–556. [PubMed: 15950161]
- (24). Wang Y, Hu WJ, Song W, Lim RKV, Lin Q. Discovery of long-wavelength photoactivatable diaryltetrazoles for bioorthogonal 1,3-dipolar cycloaddition reactions. *Org. Lett.* 2008; 10:3725–3728. [PubMed: 18671406]
- (25). Poloukhine AA, Mbua NE, Wolfert MA, Boons GJ, Popik VV. Selective labeling of living cells by a photo-triggered click reaction. *J. Am. Chem. Soc.* 2009; 131:15769–15776. [PubMed: 19860481]
- (26). (a) Holt CE, Bullock SL. Subcellular mRNA localization in animal cells and why it matters. *Science.* 2009; 326:1212–1216. [PubMed: 19965463] (b) Wu YI, Frey D, Lungu OI, Jaehrig A, Schlichting I, Kuhlman B, Hahn KM. A genetically encoded photoactivatable Rac controls the motility of living cells. *Nature.* 2009; 461:104–109. [PubMed: 19693014]



**Figure 1.** Scheme for metabolic incorporation of HAG and its subsequent functionalization by the photoinduced tetrazole-alkene cycloaddition reaction in mammalian cells: Green pentagon denotes the *in situ* generated fluorescence.

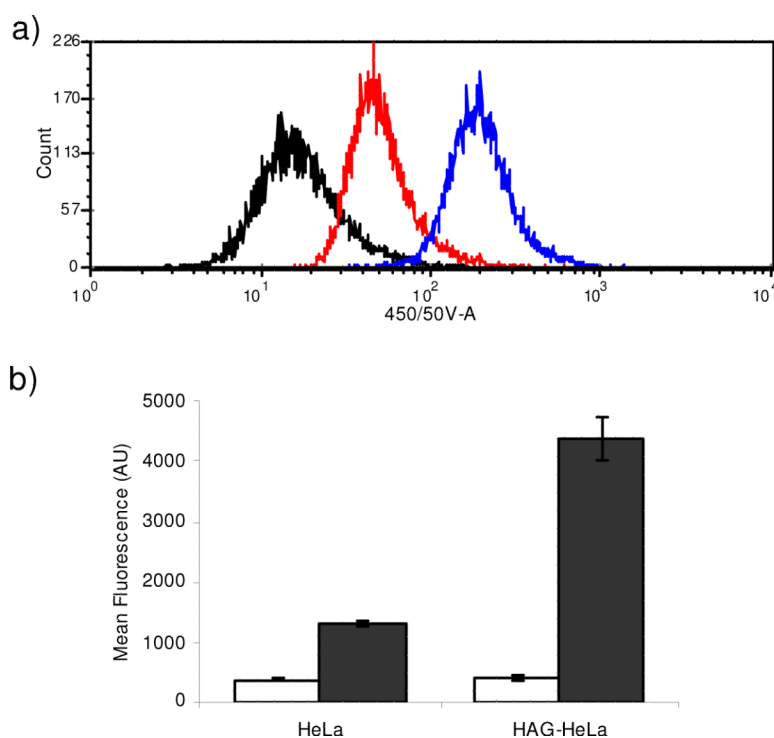
**Figure 2.**

Co-translational incorporation of HAG into newly synthesized proteins in HeLa cells and its quantification by in-gel fluorescence analysis after the photoinduced reaction with tetrazole **1**: (a) a time-course study; 1 mM of HAG (or Met control) was added to the methionine-deficient DMEM medium; (b) a concentration-dependency study. Cells were grown for 8 hr in the presence of 0.1, 0.2, 0.5, 1, 2 mM HAG or 1 mM Met. The fluorescent images were shown as the inverted images. For fluorescence quantification, the entire lanes were circled in the densitometry measurement. Three independent experiments were conducted for each incorporation condition. The trend lines were added to the plots.

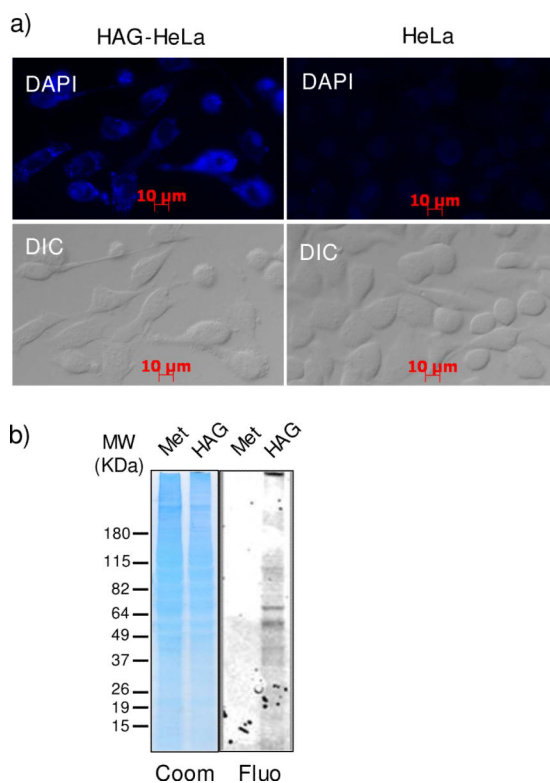
**Figure 3.**

Selective functionalization of (a) HAG-encoded  $\beta$ -gal and (b) HAG-labeled cell lysates by the tetrazole reagents via the photoinduced cycloaddition reaction. For reaction with tetrazole **1**, 0.12  $\mu$ g of HAG- $\beta$ -gal and 0.14  $\mu$ g of wt- $\beta$ -gal were used respectively in the gel analysis. For the BODIPY-tetrazole **2** mediated reaction, the fluorescent image was inverted; the fluorescence was from the green BODIPY fluorophore, not pyrazoline fluorophore. For the biotin-tetrazole **3** mediated reaction, the western blot was shown in which the biotinylated products were detected by streptavidin-alkaline phosphatase.

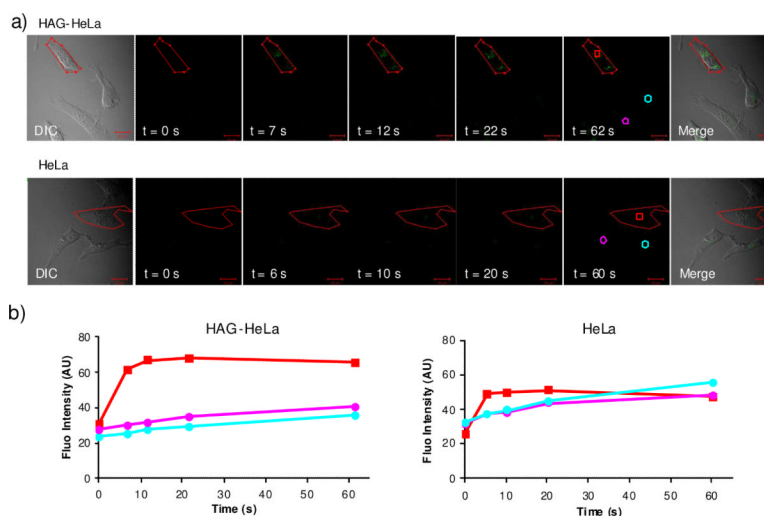


**Figure 4.**

Flow cytometry analysis of normal and HAG-labeled HeLa cells after reactions with 500  $\mu$ M tetrazole **4**: (a) Representative histograms showing populations of DMSO-treated HeLa cells (black), tetrazole **4** treated HeLa cells (red), and tetrazole **4** treated HAG-HeLa cells; (b) Bar graph representation showing the mean fluorescence for each population: white bar, DMSO control; black bar. The error bars represent standard deviations derived from three independent experiments.

**Figure 5.**

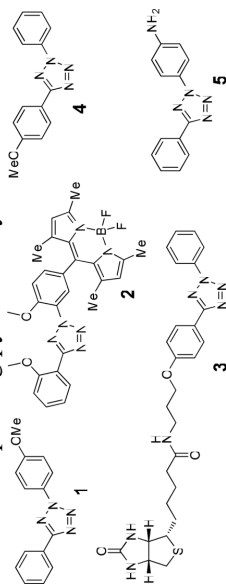
(a) Fluorescent (top) and DIC (bottom) images of HAG-HeLa and HeLa cells treated with 100  $\mu$ M tetrazole **4** for 10 min followed by 2-min photoirradiation at 302 nm. Scale bar = 10  $\mu$ m. (b) Confirmation of *in situ* protein labeling via the photoinduced reaction in HeLa cells by in-gel fluorescence analysis. The fluorescence image was inverted.

**Figure 6.**

Spatiotemporally controlled imaging of HAG-labeled proteins in live HeLa cells: a) DIC (panel 1), time-lapsed fluorescence (panels 2–6), and merged DIC/fluorescence (panel 7) images of HAG-encoded HeLa cells (top row) and normal HeLa cells (bottom row) upon two-photon illumination. All cells were treated with 200  $\mu$ M of tetrazole **5**. A 5-sec two-photon 700 nm laser was applied to the red circled area in panels 1 (sketched using the LSM-510 software). Scale bar = 20  $\mu$ m. b) Time courses of fluorescence development in the cytosolic regions in selected HeLa cells as indicated in panels 6: red square denotes the region in cells that were subjected to two-photon activation; cyan and purple circles denote the regions in the surrounding cells that were not subjected to two-photon activation.

Table 1

Structures of the various tetrazoles, second-order rate constants for selected tetrazole-4-penten-1-ol cycloaddition reactions, and photophysical properties of the corresponding pyrazoline cycloadducts.



tetrazole	$k_2$ ( $M^{-1} s^{-1}$ ) <sup>a</sup>	pyrazoline	$\lambda_{abs}$ (nm)	$\epsilon$ ( $M^{-1} cm^{-1}$ )	$\lambda_{em}$ (nm) <sup>b</sup>	$\Phi_F$ <sup>c</sup>
<b>1</b>	0.52	<b>P1</b>	354	4,200	555	0.0068
<b>4</b>	0.15	<b>P4</b>	356	5,200	501	0.080
<b>5</b>	0.79	<b>P5</b>	362	6,000	511	0.0041

See Supporting Information for details.

<sup>a</sup>The reaction was performed by irradiating a 200- $\mu$ L mixture of 100  $\mu$ M tetrazole and 10 mM 4-penten-1-ol in a quartz test tube with a handheld UV lamp at 302 nm (see ref. 19 for details).

<sup>b</sup> $\lambda_{ex}$  = 346 nm.

<sup>c</sup>Quantum yields were measured using Rhodamine 6G as the standard ( $\Phi_F$ , DAPI = 0.95 in PBS buffer).

**Table 2**Identification of HAG incorporation in  $\beta$ -galactosidase by nano-LC/MS-MS.

entry	incorporation site	fragment sequence	charge	occupancy
1	Met-1	#IDPVVLQR	+1, +2	83.7% <sup>a</sup>
2	Met-202	WSDGSYLEDDQD#WR	+2	54.1%
3	Met-246	AVLEAEVQ#CGELR	+2	64.9%
4	Met-367	HEHHPLHGQV#DEQT#VQDILL#K	+3	69.0% <sup>b</sup>
5	Met-372	HEHHPLHGQVMDEQT#VQDILLMK	+3	84.8% <sup>c</sup>
6	Met-379	HEHHPLHGQV#DEQT#VQDILL#K	+3	69.0% <sup>d</sup>
7	Met-502	SVDPSRPVQYEGGGADTTATDIICP#YAR	+3	53.4%
8	Met-655	HSDNELLHW#VALDGKPLASGEVPLDVAPQGK	+3	42.3%
9	Met-864	IDGSGQ#AITVDVEVASDTPHAR	+3	55.4%
10	Met-1043	LISEEDLN#HTGHHHHHH	+2	56.7%
11	Met-420	THG#VPMNRLTDD	+3	NA
12	Met-603	QFC#NGLVFADR	+2	NA

# denotes HAG. The occupancy was calculated using the following equation: % occupancy =  $I_{\text{HAG}} / (I_{\text{HAG}} + I_{\text{MET}})$ , where  $I_{\text{HAG}}$  and  $I_{\text{MET}}$  were ion counts for the HAG- and Met-encoded peptide fragments in the MS spectra. NA, not available.

<sup>a</sup> Averaged between the +1 and +2 charge states.

<sup>b</sup> Determined by comparing ion count of HEHHPLHGQV#DEQT#VQDILL#K over that of HEHHPLHGQVMDEQT#VQDILL#K.

<sup>c</sup> Determined by comparing ion count of HEHHPLHGQVMD EQTMVQDILL#K over that of HEHHPLHGQVMDEQTMVQDILLMK.

<sup>d</sup> Determined by comparing ion count of HEHHPLHGQV#DEQT#VQDILL#K over that of HEHHPLHGQV#DEQT#VQDILLMK.